東北大学機関リポジトリ
TOUR
Tohoku University Repository

CO2 Utilization via Direct Aqueous Carbonation of Synthesized Concrete Fines under Atmospheric Pressure

著者	Hsing Jung Ho, Atsushi Iizuka, Etsuro Shibata, Hisashi Tomita, Kenji Takano, Takumi Endo
journal or publication title	ACS Omega
volume	5
number	26
page range	15877-15890
year	2020-06-22
URL	http://hdl.handle.net/10097/00130847

doi: 10.1021/acsomega.0c00985

Creative Commons : 表示 - 非営利 - 改変禁止
http://creativecommons.org/licenses/by-nc-nd/3.0/deed.ja

This is an open access article published under a Creative Commons Attribution (CC-BY) License, which permits unrestricted use, distribution and reproduction in any medium, provided the author and source are cited.

ACS AUTHORCHOICE

ACS OMEGA

http://pubs.acs.org/journal/acsodf

Article

CO_2 Utilization via Direct Aqueous Carbonation of Synthesized Concrete Fines under Atmospheric Pressure

Hsing-Jung Ho,* Atsushi Iizuka,* Etsuro Shibata, Hisashi Tomita, Kenji Takano, and Takumi Endo

Cite This: *ACS Omega* 2020, 5, 15877−15890

Read Online

ACCESS | Metrics & More | Article Recommendations | Supporting Information

ABSTRACT: Mineral carbonation using alkaline wastes is an attractive approach to CO_2 utilization. Owing to the difference between waste CO_2 and feedstock CO_2, developing CO_2 utilization technologies without CO_2 purification and pressurization is a promising concept. This study investigated a potential method for CO_2 utilization via direct aqueous carbonation of synthesized concrete fines under atmospheric pressure and low CO_2 concentration. The carbonation reaction with different solid−liquid ratios and different concentrations of introduced CO_2 was examined in detail. Under basic conditions, a CO_2 uptake of 0.19 g-CO_2/g-concrete fines demonstrated that direct aqueous carbonation of concrete fines under atmospheric pressure and low CO_2 concentration is effective. The $CaCO_3$ concentration, degree of carbonation, and reaction mechanism were clarified. Furthermore, characterization of the carbonated products was used to evaluate ways of utilizing the carbonated products.

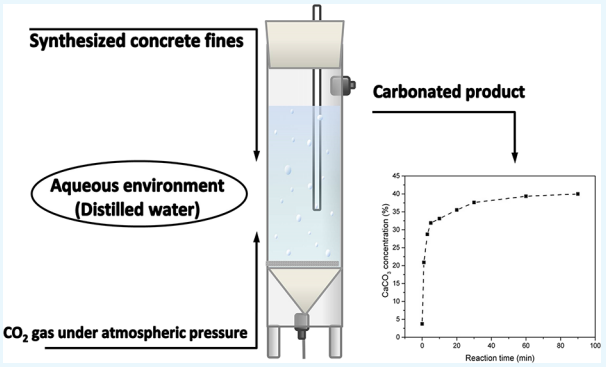

1. INTRODUCTION

Carbon capture and utilization (CCU) is one potential option for mitigating the problem of CO_2 emissions. In the CCU technology, CO_2 is regarded as feedstock to be utilized in various applications, which could simultaneously yield economic income and reduce CO_2 emissions. With consideration of requirements and situation, several CO_2 utilization technologies have been investigated. One of the problems is the difference in CO_2 purity and pressure between waste CO_2 and feedstock CO_2. Most CCU technologies require high-purity and high-pressure feedstock CO_2, while CO_2 purity is <40% in most flue gas sources.[1] Previous research has investigated the CCU technology with consideration of the difference between waste CO_2 and feedstock CO_2,[2] and one of the most promising concepts is the development of the CCU technology without CO_2 purification and pressurization.[1]

Mineral carbonation is a potential route for developing CO_2 utilization without CO_2 purification and pressurization. In this route, alkaline rocks and waste react with CO_2 to form a final product of carbonates. Rocks such as olivine,[3,4] wollastonite,[4−6] and serpentine[7] and waste such as concrete sludge,[8−10] waste concrete,[11−18] cement kiln dust,[19] fly ash,[20−25] and steel slag[26−29] are used in mineral carbonation. The main carbonation reaction of Ca-bearing and Mg-bearing materials with CO_2 is defined as follows

$$\text{alkaline rocks/waste (Ca, Mg)} + CO_2 \rightarrow \text{carbonates } (CaCO_3, MgCO_3) + \text{residues}$$

The reaction of carbonation using alkaline rocks and waste has certain advantages. Mineral carbonation is a spontaneous reaction,[30] which means it can proceed with a reasonably low energy demand. This could both save on the required energy input and introduce the possibility of the process being able to proceed without CO_2 purification and pressurization. Moreover, carbonate is more stable than other products derived from CCU applications;[31,32] hence, it also provides considerable potential regarding CO_2 sequestration. In addition, carbonates have various other applications and a huge market.[33] Therefore, the CCU technology in which carbonates are the final product has relatively huge potential in comparison to other applications and their products.

The critical problem with mineral carbonation is the slow reaction speed, although the utilization of alkaline waste for mineral carbonation might be a potential solution. It has been reported that carbonation of industrial waste can be faster than that of natural rocks.[34] In addition, it has been demonstrated that the reaction ratio and rate for waste concrete are higher than those for alkaline rocks such as wollastonite, olivine, and phlogopite.[4] One of the reasons for this can be ascribed to the different crystal structure. In alkaline rocks, calcium and

Received: March 4, 2020
Accepted: June 9, 2020
Published: June 22, 2020

Downloaded via TOHOKU UNIV on December 1, 2020 at 04:29:49 (UTC).
See https://pubs.acs.org/sharingguidelines for options on how to legitimately share published articles.

Table 1. Elemental Composition of the Synthesized Concrete Fines

element	Ca	Si	Al	Fe	S	Mg	K	Na	P	others
mass (%)	37.9	9.54	2.36	1.74	0.74	0.54	0.18	0.17	0.10	46.8

magnesium are included in the framework at the bonds between silicon and oxide,[35,36] resulting in reduced accessibility of calcium and magnesium and low calcium and magnesium extraction efficiency.

Moreover, in comparison to natural rocks, alkaline waste can sometimes contain more reactive silicates than inert silicates, e.g., the dicalcium silicate found in slags and cement. Alkaline waste also sometimes contains free oxides or hydroxides that are even more reactive than dicalcium silicate. Given alkaline waste is generally more reactive than natural rocks and usually generated near point sources of CO_2 emissions, alkaline waste has considerable potential regarding the development of carbonation without CO_2 purification and pressurization. Moreover, using alkaline waste can simultaneously reduce CO_2 emissions and mitigate the negative impact of such waste on the environment.[37] For example, concrete is one of the most popular construction materials worldwide, and waste concrete creates a major solid waste disposal problem.[38] Every year, not only fresh concrete is produced but also huge quantities of construction waste are created. In the EU, more than 450 million tons of construction and demolition (C&D) waste are generated annually.[39] The United States Environmental Protection Agency has estimated the quantity of C&D debris generated in the United States. In 2014, the total amount of C&D debris generated was 534 million tons, of which concrete accounted for 70%.[40] According to published literature, the maximum CO_2 capture potential through the formation of carbonates from C&D waste is 77−110 kg-CO_2/t.[41] Hence, it shows that mineral carbonation of construction waste has considerable potential regarding the reduction of CO_2 emissions and the increase of CO_2 utilization. Based on such information, we consider the carbonation potential of waste concrete in the United States to be approximately 28.8−41.1 million t-CO_2 annually, while the total amount of CO_2 emitted by the cement industry in the United States is estimated to be 29.4 million t-CO_2 annually.[42] Ideally, nearly 100% of CO_2 from the cement industry could be captured through carbonation by waste concrete. In addition, cement production factories produce large amounts of flue gas containing approximately 14−33% CO_2.[1,43] Therefore, the development of mineral carbonation using waste concrete represents a realistic way to both neutralize CO_2 emissions and resolve environmental problems.

As is well known, concrete is a mixture of hydrated cement (30%) and coarse and fine aggregates (70%). The reactivity of the aggregates is low because aggregates are inert rocks. Conversely, hydrated cement is a reactive alkaline material because it contains reactive free calcium hydroxide and di/tricalcium silicates. It should be noted that it is possible to derive di/tricalcium silicates from unreacted cement with water. Furthermore, calcium silicate hydrates contained in hydrated cement are known to be in the amorphous phase, which would result in moderate reactivity with CO_2. Thus, for CCU of waste concrete, crushing and separation of the concrete are needed. In an indirect CCU process, Iizuka et al. utilized actual waste concrete fines (finely crushed hydrated cement particles), i.e., a fine powdery byproduct (particle diameter: <212 μm) generated by the process of recycling an aggregate of waste concrete.[14] Vanderzee et al. also proposed aggregate recycling with CCU using concrete fines.[44] HeidelbergCement recently proposed a carbon-neutral process for cement and concrete manufacturing.[45] In the proposed concept, aggregates and sands are recycled using specifically designed processes. Two pathways for the recycling of concrete fines are mentioned: introduction to a cement kiln or carbonation with CO_2 followed by mixing to obtain cement clinker that could be crushed to obtain the final cement product. Trials of this nature are very important for achieving a circular economy for the cement and concrete industries and for avoiding the generation of unrecyclable waste.

Given this background, the promising technique of carbonation of concrete fines obtained through the recycling of aggregates should be investigated in depth. Moreover, to the best of our knowledge, our study marks the first investigation of direct carbonation of concrete fines under atmospheric pressure and low CO_2 concentration. As this represents new research, for an ideal case, we investigated the direct aqueous carbonation behavior of finely crushed hydrated cement, which simulates ideal waste concrete fines without aggregate contamination, under low CO_2 concentrations without CO_2 pressurization. It was expected that the small size of the particles of the concrete fines with relatively large available surface areas would produce greater carbonation efficiency.[15,44]

In this study, the effect of the carbonation reaction, e.g., the change of CO_2 concentration and CO_2 uptake, and the characteristics of the product, e.g., the $CaCO_3$ concentration, degree of carbonation, and formation of particles, were investigated in detail. The objectives of this paper are (1) to demonstrate the possibility of direct carbonation using concrete fines under atmospheric pressure and low CO_2 concentration, (2) to evaluate the performance of CO_2 uptake, (3) to analyze the characteristics of the final product, and (4) to make comprehensive comments regarding the potential of the technique.

2. MATERIALS AND METHODS

2.1. Materials. The concrete fines used in this study were synthesized by mixing cement (401K, Japan Cement Association, Japan) and distilled water (conductivity: 0.64 μS/cm) with a weight ratio of 100:55. The prepared cement paste was introduced into the mold (size: 18 × 22 × 4 cm^3) and cured at room temperature for 28 days, following which the mold was removed. The sample was then crushed in a crushing mill (M 20 Universal mill, IKA, Germany) and sieved (sieve size: 212 μm) to simulate the actual particle size of concrete fines, which could be obtained as a byproduct from an aggregate recycling process for further experiments.

2.2. Characterization of the Synthesized Concrete Fines. The elemental composition of the synthesized concrete fines was analyzed using inductively coupled plasma optical emission spectrometry (ICP-OES; Spectro Arcos, Spectro Analytical Instruments, Germany). A sample of approximately 100 mg of raw material was weighed and dissolved by adding 2.5 mL of HCl (35%), 1.5 mL of HF (30%), 6 mL of HNO_3 (60%), and 15 mL of H_3BO_3 (saturated solution), supplied by Fujifilm Wako Pure Chemical Corporation, at 200 °C for 2 h. Then, the obtained solution was analyzed using ICP-OES. Table 1 shows that the synthesized concrete fines comprised mainly Ca

https://dx.doi.org/10.1021/acsomega.0c00985
ACS Omega 2020, 5, 15877−15890

(37.9%), Si (9.54%), Al (2.36%), Fe (1.74%), S (0.74%), and Mg (0.54%). Thus, the concrete fines were rich in alkaline Ca, indicating their potential for reaction with CO_2 to form carbonates.

The crystalline phase of the synthesized concrete fines was characterized using X-ray diffraction (XRD; D2 Phaser, Brucker AXS, Germany) with a scan rate of 2.22°/min (Figure 1). It can

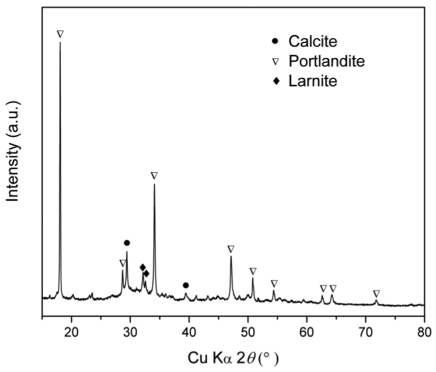

Figure 1. XRD pattern of the synthesized concrete fines.

be seen that the crystalline phase of the sample contained portlandite ($Ca(OH)_2$), calcite ($CaCO_3$), and calcium silicate (mainly larnite, Ca_2SiO_4). In addition, the concrete fines also included the amorphous phase of calcium silicate hydrates ($3CaO{\cdot}2SiO_2{\cdot}4H_2O$, etc.) gel.[14] This result is in accordance with the typical representative of hydrated cement.[46] The order of reactivity for carbonate formation would be as follows: portlandite > larnite > calcium silicate hydrates > calcium aluminate hydrates > calcite. Based on this order of reactivity, portlandite would be the main reactive component for CO_2 mineralization.

Particle size distribution was analyzed using a particle size distribution (PSD) analyzer (Microtrac MT3000 II, Nikkiso, Japan) and expressed as a particle-volume-based distribution and particle-surface-area-based distribution using isopropyl alcohol as the solvent (supplied by FUJIFILM Wako Pure Chemical Corporation). It was determined that the volumetric median diameter of the particles was 66 μm and that < 5 vol % of the particles were >212 μm. The surface-area median diameter of the particles was 7.59 μm. In addition, the volumetric mean diameter was 235.4 μm and the surface-area mean diameter was 160.1 μm.

To determine the original carbonated calcium content in the synthesized concrete fines during its preparation, the sample was analyzed using thermal gravimetric (TG) analysis (Thermoplus Evo TG 8120, Rigaku, Japan) in the temperature range of 25−1000 °C under a heating rate of 10 °C/min and an Ar flow rate of 200 mL/min. The decomposition of $CaCO_3$ that is characterized by significant weight loss occurs distinctively at temperatures of 600−800 °C. According to the weight loss within the specified temperature range, the $CaCO_3$ content can be calculated.[47] The trace of the TG analysis of the raw material is shown in Figure S1. The obvious weight loss at around 400−500 °C indicates the substantial content of $Ca(OH)_2$, which is consistent with the result of the XRD analysis.[48] The $CaCO_3$ content in the raw material was 3.73 wt %, which was determined using the following equation

$$W_{CaCO_3}\,(\text{wt }\%) = (W_{CO_2}) \times (M_{CaCO_3}/M_{CO_2}) \quad (1)$$

where W_{CaCO_3} represents the weight percent of $CaCO_3$ in the solid particles, W_{CO_2} represents the weight loss of CO_2, and M_{CaCO_3} and M_{CO_2} represent the molecular weights of $CaCO_3$ and CO_2, respectively. To clarify the Ca availability, the content of effective Ca for carbonation (36.4 wt %) was determined using the following equation

$$W_{Ca,effective}(\text{wt }\%) = W_{Ca,total} - W_{Ca,reacted} = W_{Ca,total} - W_{CaCO_3} \times (M_{Ca}/M_{CaCO_3}) \quad (2)$$

where $W_{Ca,effective}$, $W_{Ca,total}$, and $W_{Ca,reacted}$ represent the weight percent of effective Ca for carbonation in the sample, weight percent of Ca in the fresh sample, and weight percent of reacted Ca in the sample (i.e., existing as $CaCO_3$), respectively. This index assumes all unreacted Ca is available to participate in the reaction. In addition, the effective Ca can be converted to the maximum potential of CO_2 captured as $CaCO_3$, which was calculated as 0.40 g-CO_2/g-concrete fines. It must be noted that this value is the ideal maximum potential, which will decrease because of the consideration of the presence of inert aggregates and further carbonation during treatment. The reason is the main impurity in actual concrete fines is crushed aggregate, which is usually composed of silicate and limestone that are less active than hydrated cement, although they still have the capability for CO_2 capture.[49] Therefore, impurities decrease the percent of effective Ca slightly and are essentially inert in relation to the carbonation process.

2.3. Direct Aqueous Carbonation. In this study, synthesized concrete fines were carbonated using a direct aqueous carbonation method. In this method, the fine powdery concrete fines were first distributed in water in a cylindrical column reactor, and then CO_2-containing gas was introduced from the bottom of the reactor. After the direct aqueous carbonation process, carbonated powder (mixture of precipitated $CaCO_3$ and Ca-extracted concrete fines) was obtained as the final product. Although the construction and operation of the reactor are simple, the reaction itself is complicated because the reaction system involves three phases (gas, liquid, and solid). Therefore, the reaction mechanism is summarized here. The direct aqueous carbonation process using concrete fines is based on the three main steps of the reaction: (i) Ca extraction from concrete fines, (ii) CO_2 dissolution, and (iii) $CaCO_3$ precipitation.

As shown in Figure 1, the main phases of the synthesized concrete fines are crystalline $Ca(OH)_2$ and Ca_2SiO_4 and amorphous calcium silicate hydrates ($3CaO{\cdot}2SiO_2{\cdot}4H_2O$, etc.) gel. The Ca extraction step is shown as eqs 3−5. During this step, OH^- is released into the aqueous phase, which results in an increase of pH value that enhances CO_2 dissolution into solution from the gaseous phase. The extracted Ca^{2+} in the aqueous phase is used for $CaCO_3$ precipitation:

(i) Ca extraction from concrete fines

$$Ca(OH)_2 \rightarrow Ca^{2+} + 2OH^- \quad (3)$$

$$Ca_2SiO_4 + 2H_2O \rightarrow 2Ca^{2+} + SiO_2 + 4OH^- \quad (4)$$

$$3CaO \cdot 2SiO_2 \cdot 4H_2O + 6H^+ \rightarrow 3Ca^{2+} + 2SiO_2 + 7H_2O \quad (5)$$

https://dx.doi.org/10.1021/acsomega.0c00985
ACS Omega 2020, 5, 15877−15890

During the CO_2 dissolution step, as shown in eq 6, CO_3^{2-} and H^+ are released into the aqueous phase. Owing to Le Chatelier's principle, the dissolution of CO_2 is favored at a basic pH, which increases the availability of CO_3^{2-}.

(ii) CO_2 dissolution

$$CO_2 + H_2O \rightarrow H_2CO_3 \rightarrow H^+ + HCO_3^- \rightarrow 2H^+ + CO_3^{2-} \quad (6)$$

After Ca extraction and CO_2 dissolution, $CaCO_3$ is formed via precipitation. The precipitation step can be described as in eq 7.

(iii) $CaCO_3$ precipitation

$$Ca^{2+} + CO_3^{2-} \rightarrow CaCO_3 \quad (7)$$

The overall reaction can be typically formulated as the following equations

$$Ca(OH)_2 + CO_2 \rightarrow CaCO_3 + H_2O \quad (8)$$

$$Ca_2SiO_4 + 2CO_2 \rightarrow 2CaCO_3 + SiO_2 \quad (9)$$

$$3CaO{\cdot}2SiO_2{\cdot}4H_2O + 3CO_2 \rightarrow 3CaCO_3 + 2SiO_2 + 4H_2O \quad (10)$$

Based on the equations above, the Ca extracted into solution is precipitated as $CaCO_3$ and the pH value of the water is neutralized. Hence, the water used in the process as the solvent could be reused, achieving repeated water circulation.

2.4. Experimental Methods. A schematic of the direct carbonation test setup is shown in Figure 2. The reactor

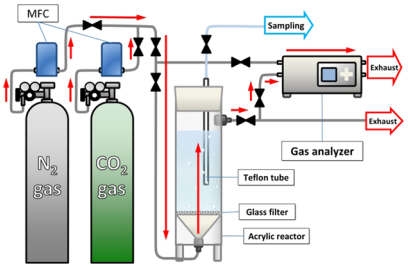

Figure 2. Schematic of the direct carbonation setup.

comprised an acrylic column, a glass filter, and a Teflon tube. The glass filter (aperture size: 5−10 μm) installed at the bottom of the acrylic column dispersed the CO_2 gas as it bubbled away. The continuous gas analyzer (EL3020 Uras 26, ABB, Germany) observed the change of CO_2 concentration and fed the information to the data logging software every second. As reported in the literature,[1] the CO_2 concentration of flue gas from a cement kiln plant is approximately 14−33%. Therefore, in this study, the CO_2 concentration was set to 14%, mixed with N_2 gas (99.99%, Taiyo Nippon Sanso Corporation) and CO_2 gas (99.99%, Taiyo Nippon Sanso Corporation), to simulate the lowest CO_2 concentration of the waste stream from cement industry at a fixed flow rate of 4000 mL/min controlled by a mass flow controller (8500 MC, Kofloc, Japan). In addition, the CO_2 concentration was also set to 5 and 30% to investigate the carbonation influence under the condition of different CO_2 purities. Before the carbonation reaction started, synthesized CO_2 was inserted into the reactor for several minutes to ensure that the CO_2 concentration in the outlet was the same as that introduced at the reaction start point. The solvent set in the column reactor in this experiment was 2 L of distilled water. The solid−liquid ratio is a variable parameter that was set as 10, 25, and 50 g/L in separate experiments. It should be noted that the solid−liquid ratio of 50 g/L represents the highest capacity for the reactor used in this experimental setup. The reaction took place at room temperature, i.e., approximately 20 ± 1 °C. After the carbonation tests, the sample was filtered through a 0.45 μm filter paper (Advantec, Japan). The solid sample obtained from the filtration process was analyzed using TG, XRD, PSD, and ICP-OES analyses. The liquid sample obtained from the filtration was analyzed based on pH and ICP-OES. Based on these analyses, the advanced results were determined using several calculations.

2.5. Estimation of CO_2 Uptake and Degree of Carbonation under Basic Conditions. As described in Section 2.3, gaseous CO_2 is first dissolved into solution, and then part of the dissolved CO_2 is fixed in the solid phase as $CaCO_3$. Thus, over time, the following equation is true

$$CO_2\text{uptake (g} - CO_2) = \text{dissolved } CO_2\text{in solution (g} - CO_2) + CO_2\text{as } CaCO_3\text{(g} - CO_2) \quad (11)$$

where CO_2 uptake means the total amount of CO_2 absorbed from the gaseous phase. It is considered that water in the direct aqueous carbonation process could be used repeatedly in further carbonation processes. Thus, the CO_2 fixed in the solid phase as $CaCO_3$ will be more important as an indicator for CO_2 sequestration. However, to describe and consider the total reaction system, CO_2 uptake is also a useful indicator.

To evaluate the CO_2 uptake capacity, the ideal gas law is used to calculate the amount of CO_2 uptake

$$CO_2\text{uptake(g} - CO_2) = \frac{(\Delta V_{CO_2} \times P)}{RT} \times M_{CO_2} \quad (12)$$

where ΔV_{CO_2} represents the volume of captured CO_2 (L) and P = 1.01 bar, R = 0.083 bar L K^{-1} mol^{-1}, T = 293 K, and M_{CO_2} = 44.01 g/mol. Moreover, ΔV_{CO_2} can be calculated as follows

$$\Delta V_{CO_2}(L) = \int_0^t F_{total} \times \frac{(C_{CO_2,i} - C_{CO_2,t})}{100}\, dt \quad (13)$$

where F_{total} represents the total flow rate (L/min) and $C_{CO_2,i}$ and $C_{CO_2,t}$ denote the CO_2 gas concentration (%) at the start point and at time t (min), respectively.

To estimate the amount of CO_2 fixed in the solid phase as $CaCO_3$, qualification of the $CaCO_3$ content in the solid is needed. The weights of the concrete fines feed and the carbonated solid are supposed to be the same. As mentioned previously, the $CaCO_3$ content can be analyzed using TG analysis and calculated using eq 1. Therefore, the amount of CO_2 captured as $CaCO_3$ can be calculated as follows

$$CO_2\text{as } CaCO_3\text{(g} - CO_2) = \frac{W_{CaCO_3,f} - W_{CaCO_3,i}}{100} \times \frac{M_{CO_2}}{M_{CaCO_3}} \times W_{solid} \quad (14)$$

where $W_{CaCO_3,i}$ represents the initial amount of $CaCO_3$ in the raw material and $W_{CaCO_3,f}$ represents the amount of $CaCO_3$ in the carbonated products after carbonation. To interpret the

https://dx.doi.org/10.1021/acsomega.0c00985
ACS Omega 2020, 5, 15877−15890

carbonation efficiency with variable parameters, the degree of carbonation was calculated using eq 15

$$\text{degree of carbonation}(\%) = \frac{\Delta W_{\text{Ca, effective}}}{W_{\text{Ca, effective}}} \times 100 \quad (15)$$

where $\Delta W_{\text{Ca, effective}}$ represents the change of weight percent of effective Ca for carbonation in the sample.

3. RESULTS AND DISCUSSION

3.1. Carbonation Reaction under Basic Conditions.

This section summarizes the carbonation behavior of the synthesized concrete fines under basic conditions of 14% CO_2 and a solid−liquid ratio of 10 g/L.

The temporal variations of Ca and Si concentration in solution, pH in solution, and CO_2 concentration at the outlet of the reactor are shown in Figures 3−5, respectively. The

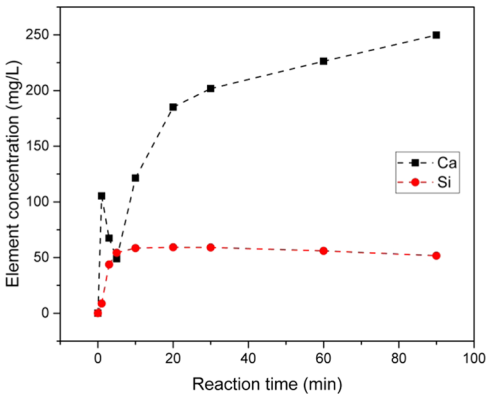

Figure 3. Temporal variation of Ca and Si concentration under basic conditions.

concentrations of Ca, Si, and other elements were measured by ICP-OES. Under the stated conditions, the Ca concentration increased rapidly to over 100 ppm, then decreased, and finally increased again, before eventually leveling off at around 250 ppm (Figure 3). It is considered that the Ca concentration in solution is determined by the balance of the rates of Ca extraction (eqs 3−5) and $CaCO_3$ precipitation (eq 7). In the initial reaction stage, Ca extraction from the surface of the fresh concrete fines is dominant, which prompts $CaCO_3$ precipitation that results in a decrease of the Ca concentration. In a later stage of the reaction, the rates of Ca extraction and $CaCO_3$ precipitation must be balanced at the equilibrium Ca concentration of the system. At the reaction time of 90 min, Ca concentration was approximately 250 ppm, which is considered close to the saturated Ca concentration for a Ca−H_2O−CO_2 system based on the literature data.[50,51] During the reaction, the Si concentration in solution increased and then leveled off at approximately 50 ppm. It should be noted that the concentrations of elements such as S, K, and Mg were approximately 34, 7.7, and 4.9 mg/L, respectively, while that of toxic elements such as Cr was <0.19 mg/L and those of Cd, Fe, and Pb were <0.01 mg/L.

The temporal variation of pH during the carbonation reaction is shown in Figure 4. First, the concrete fines are dissolved and Ca^{2+} and OH^- are released into the aqueous phase, as indicated by eqs 3−5, and the results are consistent with the change of Ca^{2+} shown in Figure 3. The pH value increased directly to almost 12 within 10 min, which is near the pH value of the

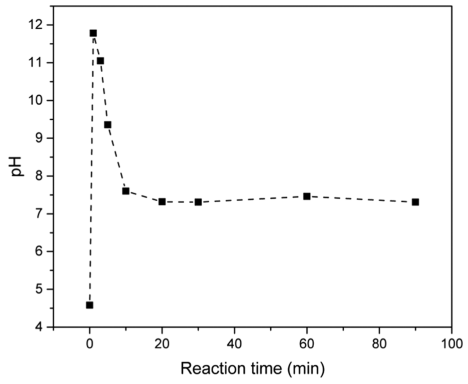

Figure 4. Temporal variation of pH under basic conditions.

saturated $Ca(OH)_2$ solution, i.e., approximately 12.5, which proves that the concrete fines are dissolved remarkably well.[52] Equation 6 indicates that higher pH can promote the reaction of CO_2 dissolution. As the pH value increases, the CO_2 concentration is reduced significantly because a considerable amount of CO_2 gas is dissolved into the aqueous state. Then, the OH^- is consumed owing to the CO_2 dissolution reaction that resulted in the decrease of the pH value, and the reaction reaches equilibrium. In addition, given the elemental composition and the pH value, Ca is precipitated as $CaCO_3$ and the pH is neutralized by the reaction of Ca extraction and CO_2 dissolution. Thus, the water used as the solvent could be reused repeatedly.

The temporal variation of CO_2 concentration at the outlet of the reactor is shown in Figure 5. The results indicate that CO_2 is

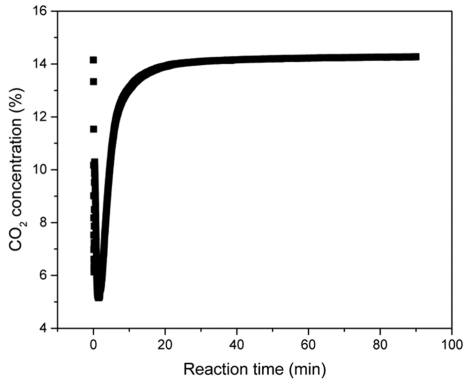

Figure 5. Temporal variation of CO_2 concentration under basic conditions.

absorbed initially, as evidenced by the sharp decrease in CO_2 concentration. The reason can be explained by referring to eq 6 and Figure 4. As the reaction starts, the pH value increases immediately and the CO_2 dissolution reaction is enhanced, which correspondingly results in a decrease of the CO_2 concentration. Then, the CO_2 concentration becomes stable after approximately 30 min.

In addition, the results of the variation of the CO_2 concentration can be used to calculate CO_2 uptake using eqs 12 and 13. The results of the XRD analysis of both the raw concrete fines and the final carbonated products are shown in Figure 6. It can be seen that the peak of portlandite is reduced and that the peak of calcite is increased, indicating significant carbonation of the raw concrete fines. The temporal variation of $CaCO_3$ concentration via direct carbonation under the basic

https://dx.doi.org/10.1021/acsomega.0c00985
ACS Omega 2020, 5, 15877−15890

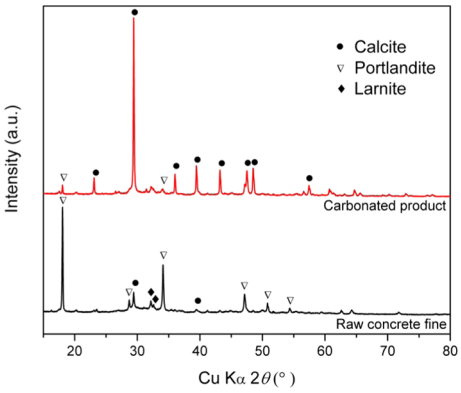

Figure 6. Comparison of XRD patterns of synthesized concrete fines and carbonated products under basic conditions.

conditions of 14% CO_2 and 10 g/L is shown in Figure 7. Based on eq 1, the amount of $CaCO_3$ can be obtained. The $CaCO_3$

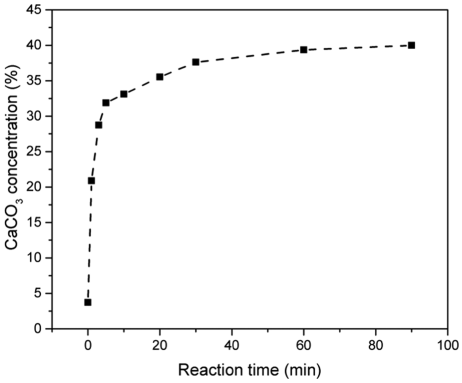

Figure 7. Temporal variation of $CaCO_3$ concentration under basic conditions.

concentration increased tremendously within the first 10 min, following which it became stable after approximately 30 min, consistent with the previous results. The $CaCO_3$ concentration reached approximately 40 wt % at 90 min, and the degree of carbonation was 39.9%, according to eq 15. In addition, based on eq 12, the CO_2 uptake was calculated as 3.71 g-CO_2 and 0.19 g-CO_2/g-concrete fines. Compared to previous research, this CO_2 uptake efficiency is greater than both direct carbonation using bauxite residue under atmospheric CO_2[53] and aqueous carbonation using coal fly ash under ambient conditions[54] and similar to direct carbonation using steelmaking slag at 100 °C and 10 bar.[55] Moreover, the total captured CO_2 includes not only that captured as $CaCO_3$ but also that captured in the aqueous phase. To elucidate the mechanism of CO_2 capture, the relationship between the CO_2 captured as $CaCO_3$ and that captured in the aqueous phase with reaction time is shown in Figure 8. In making the CO_2 concentration 14% at the start of the reaction, CO_2 was introduced before the reaction commenced, part of which was captured. After the start of the reaction, almost all of the absorbed CO_2 was captured as $CaCO_3$, and it is revealed that the reaction rate of carbonation is fast in the initial stage of the reaction. However, after 5 min, it can be seen that the total amount of CO_2 captured continued to increase but that the amount of CO_2 captured as $CaCO_3$ began to level off. Thus, most of the captured CO_2 was captured in the aqueous phase but was not precipitated as $CaCO_3$ after

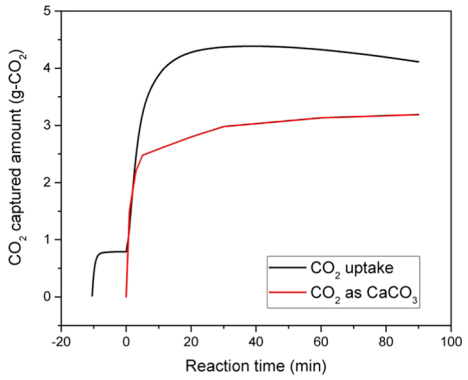

Figure 8. Relationship between CO_2 uptake and CO_2 as $CaCO_3$ under basic conditions.

approximately 5 min. At around 90 min, the amount of CO_2 captured as $CaCO_3$ was approximately 3.19 g-CO_2.

3.2. Carbonation Reaction with Different Solid−Liquid Ratios. Section 3.1 presents the results obtained under basic conditions. The solid−liquid ratio is a crucial parameter known to have a significant effect on both reaction efficiency and mineral carbonation.[56] Hence, in this section, the influence on carbonation of different solid−liquid ratios (i.e., 10, 25, and 50 g/L) is also discussed in detail.

The temporal change of Ca concentration with different solid−liquid ratios is illustrated in Figure 9. In the initial stage of

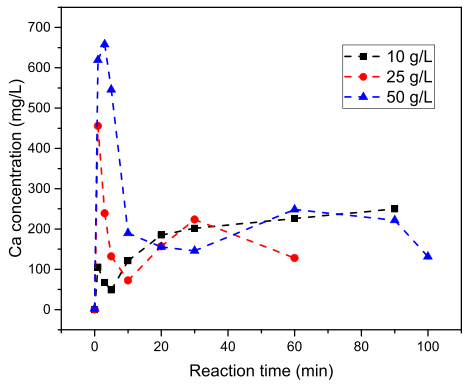

Figure 9. Temporal variation of Ca concentration under different solid−liquid ratios.

the reaction, Ca concentration increased, and the Ca concentration within 3 min was higher with a higher solid−liquid ratio. Moreover, the lower the solid−liquid ratio, the earlier the Ca concentration decreased. This is because an increase in the solid−liquid ratio means more Ca can be extracted into the aqueous phase. In addition, it is worth mentioning that the saturated Ca concentration for $Ca(OH)_2$ was approximately 860 mg/L.[57] After the initial stage of the reaction, the Ca concentration decreased sharply and then leveled off after approximately 10 min.

The relationship between the pH value and reaction time during the direct carbonation reaction is shown in Figure 10. The pH value increased considerably in the initial stage of the reaction. With a solid−liquid ratio of ≥25 g/L, the observed maximum pH was >12. Then, the pH value decreased with time and eventually became stable. The reactions reached equilibrium when the pH value was approximately 7. As shown in Figure 10, the time for the reaction to reach equilibrium was

https://dx.doi.org/10.1021/acsomega.0c00985
ACS Omega 2020, 5, 15877−15890

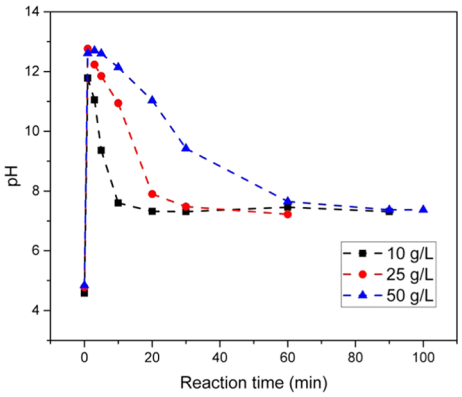

Figure 10. Temporal variation of pH under different solid−liquid ratios.

longer for the higher solid−liquid ratios, which could be attributed to the limited supply of CO_2 into the reaction solution. The rate of CO_2 introduction in the bubbled gas was 1.03 g-CO_2/min under all conditions, and the dissolution efficiency was not 100%. A larger amount of Ca was extracted under the condition of a higher solid−liquid ratio, and thus neutralization by CO_2 required longer.

The temporal variation of CO_2 concentration with different solid−liquid ratios is presented in Figure 11. The results show

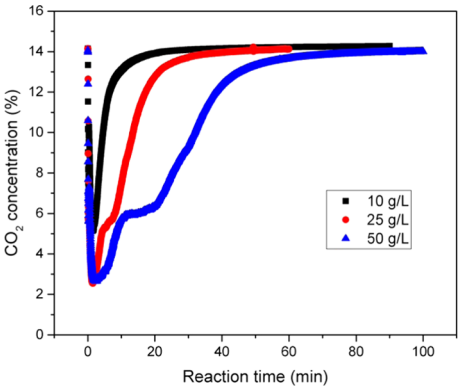

Figure 11. Temporal variation of CO_2 concentration under different solid−liquid ratios.

that under all conditions, the CO_2 concentration decreased markedly first and then increased again as reaction time elapsed. In addition, when the solid−liquid ratio was higher, the required reaction time before the rise was longer. Based on the results, the CO_2 uptake (absorbed CO_2, i.e., the sum of dissolved CO_2 and CO_2 as $CaCO_3$) with different solid−liquid ratios was calculated, as presented in Table 2. With an increase of the solid−liquid ratio, the amount of CO_2 uptake is increased, indicating that more Ca is available to capture CO_2 and to form $CaCO_3$. In addition, the CO_2 uptake efficiency (g-CO_2/g-concrete fines) is not that different (i.e., slightly higher with a higher solid−liquid ratio). This indicates that the Ca extraction rate, i.e., the extracted Ca per unit amount of concrete fines, is similar under all of the solid−liquid ratio conditions studied. In addition, the time required to reach equilibrium was shorter when the solid−liquid ratio was lower. Considering the different requirements and conditions (e.g., limited reaction time or higher CO_2 uptake efficiency), a higher (lower) solid−liquid ratio and a longer (shorter) reaction time led to slightly higher (lower) CO_2 uptake efficiency. Both sets of conditions have certain advantages that will be considered. Specifically, a higher solid−liquid ratio is better for industrial implementation. A solid−liquid ratio of 100 g/L (and higher) was tested as part of the research, but the column reactor became choked by too much precipitated solid. To address this problem, we will consider designing a reactor with larger capacity for simulating industrial implementation.

Table 2. CO_2 Uptake and CO_2 Uptake Efficiency with Different Solid−Liquid Ratios

	SL ratio (g/L)		
	10	25	50
CO_2 uptake (g-CO_2)	3.71	10.0	21.4
CO_2 uptake efficiency (g-CO_2/g-concrete fines)	0.19	0.20	0.22

Figure 12 shows the temporal variation of the $CaCO_3$ concentration of carbonated concrete fines under different

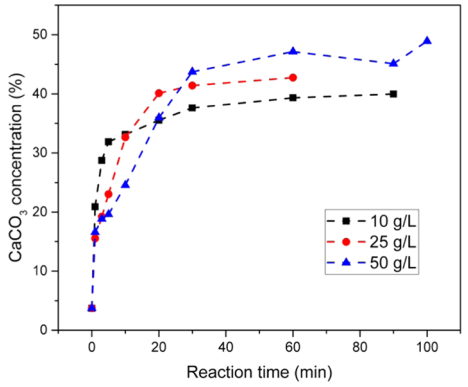

Figure 12. Temporal variation of $CaCO_3$ concentration under different solid−liquid ratios.

solid−liquid ratios. The $CaCO_3$ concentration increased more slowly for higher solid−liquid ratios, consistent with the results mentioned above; however, the final $CaCO_3$ concentration under lower solid−liquid ratio conditions was lower than that under higher solid−liquid ratio conditions. At the reaction time of 60 min, $CaCO_3$ concentrations with solid−liquid ratios of 10, 25, and 50 g/L were 39.3, 42.8, and 47.1 wt %, respectively. At 100 min, the $CaCO_3$ concentration under conditions of 50 g/L was 48.9 wt %. The temporal variation of the degree of carbonation with different solid−liquid ratios was also calculated. At the reaction time of 60 min, the degrees of carbonation with solid−liquid ratios of 10, 25, and 50 g/L were 39.2, 43.0, and 47.9%, respectively. The amounts of CO_2 captured as $CaCO_3$ per unit concrete fines with solid−liquid ratios of 10, 25, and 50 g/L were 0.16, 0.17, and 0.20 g-CO_2/g-concrete fines, respectively, as shown in Table 3.

We conducted a PSD analysis to investigate the influence of carbonation on the PSD of carbonated products. The PSD of the carbonated products under solid−liquid ratios of 10, 25, and 50 g/L is shown in Figure 13a−c, respectively. The actual values of the volumetric median diameter were as follows: 87.1 μm (10 min), 98.9 μm (30 min), 95.6 μm (60 min), and 82.8 μm (90 min) under a solid−liquid ratio of 10 g/L; 64.7 μm (10 min), 56.6 μm (30 min), and 72.5 μm (60 min) under a solid−liquid ratio of 25 g/L; and 72.4 μm (10 min), 58.8 μm (30 min), 60.7 μm (60 min), and 32.9 μm (100 min) under a solid−liquid ratio

https://dx.doi.org/10.1021/acsomega.0c00985
ACS Omega 2020, 5, 15877−15890

Table 3. Amount of CO_2 Captured as $CaCO_3$ and Dissolved in the Aqueous Phase with Different Solid−Liquid Ratios

solid−liquid ratio (g/L)	CO_2 uptake efficiency (g-CO_2/g-concrete fines)	CO_2 captured as $CaCO_3$ (g-CO_2/g-concrete fine)	CO_2 dissolved in aqueous (g-CO_2/g-concrete fine)
10	0.19	0.16	0.03
25	0.20	0.17	0.03
50	0.22	0.20	0.02

of 50 g/L. It can be seen that the average particle size of the carbonated products was larger than that of the raw synthesized concrete fines. In addition, the peak of the smaller particle size increased as reaction time elapsed. The trend is clearer in the case of the higher solid−liquid ratios. In addition, with an increase of the solid−liquid ratio, the average particle size reduced and the peak of the smaller particle size increased, as shown in Figure 13d. Two main mechanisms could explain the derived results. The first mechanism reflects that $CaCO_3$ is formed on the surface of the particles in the direct carbonation reaction. However, $CaCO_3$ is not hard and it could easily become detached. Therefore, with an increased solid−liquid ratio, the probability of particle collisions would increase, which could cause the $CaCO_3$ on the surface of the particles to become detached and form high-$CaCO_3$-concentration fine particles. The second mechanism reflects that with an increased solid−liquid ratio, the Ca^{2+} concentration would increase to an oversaturated state, becoming evenly dispersed within the aqueous solution. Therefore, $CaCO_3$ is not only formed on the surface of the particles surface but it also undergoes a nucleation reaction in the aqueous phase to form high-$CaCO_3$-concentration fine particles.

To elucidate the difference between large and small carbonated particles, TG analysis was used to demonstrate the $CaCO_3$ concentration of large and small carbonated particles based on eq 1. According to the PSD analysis, large and small carbonated particles could be distinguished based on a threshold value of 53 μm (Table 4). The carbonated particles were sieved (threshold: 53 μm) to distinguish large and small carbonated particles. The $CaCO_3$ concentrations of small particles under solid−liquid ratios of 10, 25, and 50 g/L were 58.3, 57.5, and 64.2 wt %, respectively. The $CaCO_3$ concentrations of large particles under solid−liquid ratios of 10, 25, and 50 g/L were 26.1, 26.2, and 26.7 wt %, respectively. Clearly, the $CaCO_3$ concentration of large carbonated particles was notably lower than that of small particles. It indicates that fine carbonated particles are formed by detachment of large carbonated particles and the nucleation reaction in the Ca^{2+}-saturated aqueous solution. Therefore, the results confirm that small carbonated particles have higher $CaCO_3$ concentrations than large carbonated particles, reflecting the aforementioned reaction mechanisms.

The tendency reported in previous papers differs from that of this study.[20,21,58] The Ca extraction step is the rate-controlling step that would disturb the reaction in previous studies. However, in this study, CO_2 dissolution is more critical than the other reaction steps because of the low concentration of CO_2 introduced under atmospheric pressure and the high activity of the synthesized concrete fines (without aggregate contamination), suggesting that CO_2 dissolution is the limiting step in the direct carbonation process. Owing to the fast Ca extraction step, many Ca^{2+} and OH^- are released, as demonstrated in Figures 9 and 10. In addition, the tendency of the effect of the solid−liquid ratio is different compared to previous results obtained using metal waste and fly ash in mineral carbonation.[20,21,58] Ca extraction efficiency is improved when reducing the solid−liquid ratio because of the dilution effect (i.e., a larger volume of solution can increase Ca solubility).[58] The reason can be ascribed to the slow CO_2 dissolution reaction and the particle collision effect, which also plays a major role in this reaction, as demonstrated by the results of the PSD and TG analyses. Hence, when the solid−liquid ratio is high, more OH^- is released, more CO_2 can be captured, the probability of particle collisions is increased, and both CO_2 uptake efficiency and $CaCO_3$ concentration will be correspondingly higher. The result is in accordance with the previous literature on the direct carbonation of alkaline materials, which described the occurrence of the cleavage of precipitated carbonates from the particle surface.[59] A report in the literature on the indirect carbonation of MSWI fly ash indicated that a higher solid−liquid ratio resulted in a smaller particle size of the derived carbonated products, as revealed in our results.[60] The particle size of the final carbonated products in this study is larger than that reported in previous papers based on direct carbonation of argon oxygen decarburization (AOD) slag (D_{50}: 41.1 μm),[61] indirect carbonation of concrete sludge (range: 3−30 μm), and indirect carbonation of steel converter slag (range: 0.1−4 μm).[8,62] The reason is direct carbonation of AOD slag is enhanced with ultrasound, while indirect carbonation uses acidic or alkaline agents to dissolve the solid sample completely; therefore, the precipitated carbonates are finer than the carbonated products obtained from direct aqueous carbonation.

Several kinetic models such as the shrinking core model and surface coverage model are widely used to determine reaction kinetics.[63−65] However, both models assume that the reaction occurs only at the surface of the unreacted core and the unreacted surface. Therefore, in our opinion, these models are unsuitable in relation to the direct carbonation of concrete fines and thus conventional kinetic models were not considered in this study.

3.3. Carbonation Reaction with Different Concentrations of Introduced CO_2. The carbonation reaction under different concentrations of introduced CO_2 is interesting. Therefore, this section compares the results obtained with concentrations of introduced CO_2 of approximately 5, 14, and 30%, which are representative of the CO_2 emission sources of boiler exhaust gas, the minimum CO_2 concentration of cement kiln plant flue gas, and around the maximum CO_2 concentration of cement kiln plant flue gas, respectively,[1] under conditions of a solid−liquid ratio of 10 g/L.

The temporal variation of Ca concentration with different concentrations of introduced CO_2 is shown in Figure 14. In the initial stage of the reaction, Ca is extracted based on eqs 3−5, and thus the Ca concentration achieved with 5% CO_2 was higher in comparison to 14 and 30% CO_2. The reason is the balance of CO_2 supply and Ca extraction. When the CO_2 was 5%, in comparison to Ca extraction, the CO_2 supply was limited, which resulted in a higher Ca concentration. According to eq 7, the extracted Ca reacts with CO_3^{2-} to form $CaCO_3$, which reduces the Ca concentration. In the later stages of all reactions, the Ca

https://dx.doi.org/10.1021/acsomega.0c00985
ACS Omega 2020, 5, 15877−15890

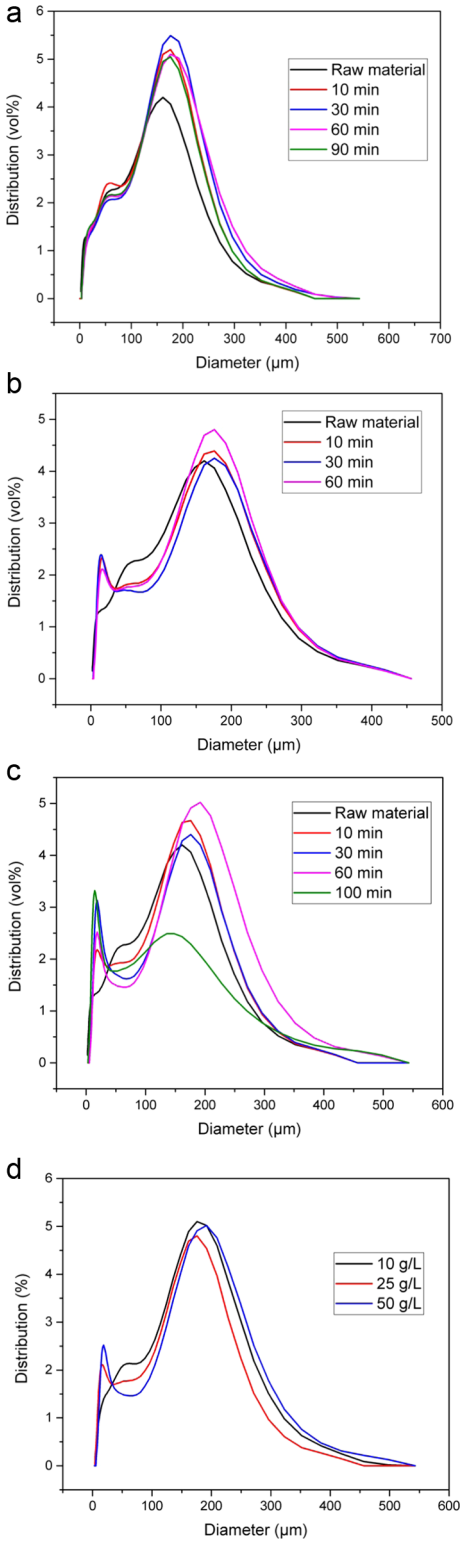

Figure 13. (a) Particle size distribution of the carbonated products at 10 g/L. (b) Particle size distribution of the carbonated products at 25 g/L. (c) Particle size distribution of the carbonated products at 50 g/L. (d) Particle size distribution of the carbonated products under different solid−liquid ratios at 60 min.

concentration increased with time, with that under the condition of 30% CO_2 increasing the most. The reason might be the different equilibrium Ca concentration under different CO_2 partial pressure. Under a higher CO_2 pressure, the saturated Ca concentration is higher. According to the ideal Ca−H_2O−CO_2 system calculated based on literature data, the saturated Ca concentration of 30% CO_2 is the highest, i.e., 178 mg/L, followed by 14% CO_2 (138 mg/L) and 5% CO_2 (97.5 mg/L).[50,51]

Table 4. $CaCO_3$ Concentrations of Large and Small Carbonated Particles

solid−liquid ratio (g/L)	10		25		50	
diameter (μm)	<53	>53	<53	>53	<53	>53
$CaCO_3$ concentration (wt %)	58.3	26.1	57.5	26.2	64.2	26.7

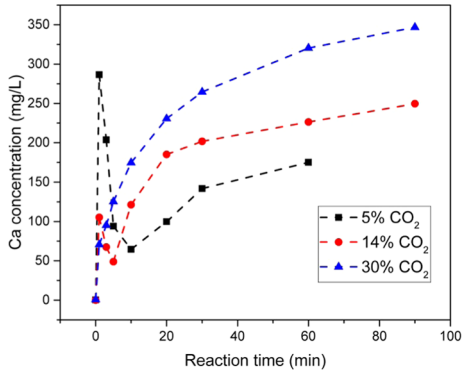

Figure 14. Temporal variation of Ca concentration under different concentrations of introduced CO_2.

The results of the pH value with 5, 14, and 30% CO_2 are shown in Figure 15. In the initial stage of the reaction, the pH value increased according to eqs 3−5. In the cases with 5 and 14% CO_2, the pH value reached its highest point at the reaction time of approximately 1 min, corresponding to Figure 14 and demonstrating the temporal variation of Ca extraction, following which the pH value of the 14% CO_2 case fell faster than the 5% CO_2 case. In an alkaline environment, CO_2 is favored for capture; therefore, the 5% CO_2 case, in which the pH value drops slowly, has a greater capacity to capture more CO_2 than the 14% CO_2 case. The pH value of the 30% CO_2 case was more stable and lower than the 5 and 14% CO_2 cases. The reason might be that the higher concentration of introduced CO_2 caused more CO_2 to be dissolved, meaning that additional H^+ was obtained. It might indicate that the amount of concrete fines was so small that the reaction of Ca extraction was feeble,

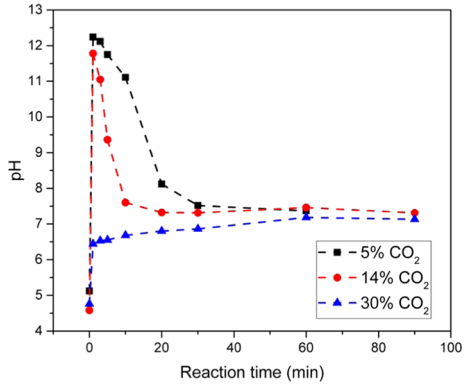

Figure 15. Temporal variation of pH under different concentrations of introduced CO_2.

https://dx.doi.org/10.1021/acsomega.0c00985
ACS Omega 2020, 5, 15877−15890

resulting in the low pH value and the low CO_2 uptake in the 30% CO_2 case. In other words, the solid−liquid ratio should be increased in the 30% CO_2 case, consistent with the results presented in Section 3.2.

The results of CO_2 concentration at the outlet of the carbonation reactor under conditions of 5, 14, and 30% CO_2 are shown in Figure 16. The results show that CO_2 was absorbed in

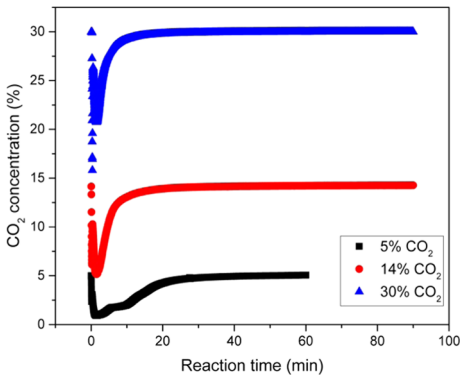

Figure 16. Temporal variation of CO_2 concentration under different concentrations of introduced CO_2.

different CO_2 concentrations. Based on these results, the CO_2 uptake efficiency was calculated using eqs 12 and 13. The CO_2 uptake efficiency with 5% CO_2 was 0.22 g-CO_2/g-concrete fines, which was higher than that of the cases with 14 and 30% CO_2, i.e., 0.19 and 0.15 g-CO_2/g-concrete fines, respectively. The amounts of CO_2 captured as $CaCO_3$ per unit concrete fines with solid−liquid ratios of 10, 25, and 50 g/L were 0.16, 0.16, and 0.15 g-CO_2/g-concrete fines, respectively, as shown in Table 5. Moreover, the $CaCO_3$ concentration of the final products also had the same trend, as shown in Figure 17. It might be explained by the fact that when the CO_2 concentration is increased, a higher solid−liquid ratio is needed, which can be proved by referring to Figure 15. When the CO_2 concentration increases, in comparison to that of the Ca extraction reaction, the amount of CO_2 dissolved is too high and the resulting pH is too low. In other words, the Ca extraction is not sufficient in this case. Based on eq 6, CO_2 dissolution is favored in an alkaline environment. Furthermore, the lower solution pH under a higher CO_2 concentration is not favorable for $CaCO_3$ precipitation because of the lower CO_3^{2-} concentration. Hence, when the CO_2 concentration is increased and the solid−liquid ratio is held constant, the CO_2 uptake efficiency and the $CaCO_3$ concentration will both be lower.

The results presented in this section demonstrate that the effectiveness of gas with a higher CO_2 concentration is not enhanced when the solid−liquid ratio is held constant in a carbonation reaction. Moreover, the findings elucidate the potential regarding mineral carbonation of concrete fines for CO_2 utilization with a low CO_2 concentration or a high solid−

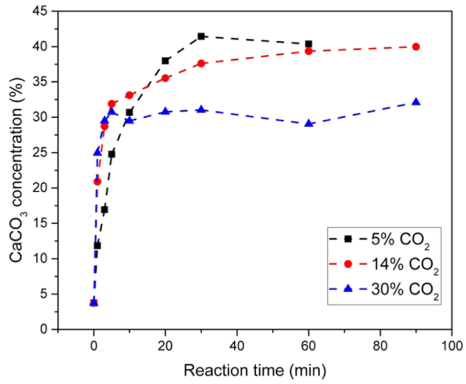

Figure 17. Temporal variation of $CaCO_3$ concentration under different concentrations of introduced CO_2.

liquid ratio, which is very meaningful and worthy of exploration. The results suggest great opportunity to develop mineral carbonation of concrete fines in reaction with several possible types of flue gas without need for CO_2 pressurization.

3.4. Characterization of Carbonated Concrete Fines.

To consider the stability or recycling applications of the carbonated concrete fines in this direct carbonation method, characterization of the carbonated materials was conducted.

The elemental composition of the carbonated products was analyzed using ICP-OES. The reaction times of the carbonated products with solid−liquid ratios of 10, 25, and 50 g/L under conditions of 14% CO_2 were 90, 60, and 100 min, respectively (Table 6). It proves that the elemental compositions of the carbonated products derived with different solid−liquid ratios were similar. Moreover, the composition of toxic elements such as Cr, Cd, and Pb was <0.01 mg/L.

Table 6. Elemental Composition of the Carbonated Products

element (%)	10 g/L	25 g/L	50 g/L
Ca	32.2	31.0	31.5
Si	7.43	7.45	8.29
Al	2.20	2.10	2.22
Fe	1.57	1.47	1.44
S	0.40	0.37	0.37
Mg	0.51	0.46	0.42
K	0.09	0.05	0.08
Na	0.05	0.04	0.07
P	0.09	0.08	0.08

A scanning electron microscopy image of the final carbonated product showing examples of the formed particles is presented in Figure S2. The image indicates that $CaCO_3$ was truly precipitated as a cubic shape on the particle surface.

To consider stock safety and to develop a method for utilization of carbonated products obtained from concrete fines, the toxicity characteristic must be clarified. The leaching

Table 5. Amount of CO_2 Captured as $CaCO_3$ and Dissolved in the Aqueous Phase with Different Concentrations of Introduced CO_2

CO_2 (%)	CO_2 uptake efficiency (g-CO_2/g-concrete fines)	CO_2 captured as $CaCO_3$ (g-CO_2/g-concrete fines)	CO_2 dissolved in aqueous (g-CO_2/g-concrete fines)
5	0.22	0.16	0.06
14	0.19	0.16	0.03
30	0.15	0.12	0.03

https://dx.doi.org/10.1021/acsomega.0c00985
ACS Omega 2020, 5, 15877−15890

behavior of carbonated products can be determined using the toxicity characteristic leaching procedure (TCLP). In this test, the carbonated products were leached under the conditions of the TCLP and toxic elements such as As, Ba, Cr, and Pb were analyzed. Moreover, as Cr is the most critical toxic element in waste concrete and concrete fines, it is critical to analyze the Cr concentration under the TCLP. The results showed that the concentrations of As, Ba, Cr, and Pb were approximately 0.01, 1.21−1.79, 0.17−0.20, and 0.02 mg/L, respectively, when the solid−liquid ratios of the carbonated products were 10, 25, and 50 g/L. All of these concentrations are well below the TCLP standard values. Therefore, as the carbonated products meet the hazardous specifications, they could possibly be utilized in various applications.

It should be noted that the particle distribution of the carbonated concrete fines did not change from before carbonation under the lower solid−liquid ratio, whereas it became smaller under the higher solid−liquid ratios. Thus, in consideration of recycling applications that might require a certain PSD, the particle size of the concrete fines would have to be regulated.

The $CaCO_3$ concentration of the final carbonated products under different solid−liquid ratios and concentrations of introduced CO_2 was approximately 32.1−48.9 wt %. The graph of the TG analysis of the final carbonated product under a solid−liquid ratio of 50 g/L and an introduced CO_2 concentration of 14% is shown in Figure S1. Between the temperatures of 600 and 800 °C, the weight loss of the final carbonated product was significantly greater than that of the raw material, which proves the increment of $CaCO_3$.

In addition, this study considered possible applications of the carbonated products. The obvious mode of utilization is CO_2 sequestration. However, the carbonated products could also be mixed with fine aggregates or asphalt filler for construction purposes,[66,67] or used as an additive for soils.[25,68] Although it would require further improvement in the purity of the carbonated products, substitution for precipitated $CaCO_3$ could also be a possible application. In addition, despite reasonably limited demand, utilization of concrete minerals[69−77] and/or $CaCO_3$ for water or gas purification could be a further option. In future work, we will consider further exploration of promising applications for the carbonated products.

4. CONCLUSIONS

This study investigated CO_2 utilization via mineral carbonation using synthesized concrete fines from an aggregate recycling process under atmospheric pressure, which makes possible the avoidance of the difficulties of CO_2 pressurization. The method examined has potential for development of a circular economy for the cement and concrete industries.

Analysis of the characteristics of the concrete fines showed that the content of effective Ca for carbonation was 36.4 wt % and that the main crystalline phases were portlandite, calcite, and larnite. The results of the carbonation reaction under basic conditions showed that CO_2 uptake was 3.71 g-CO_2 and that almost all of the absorbed CO_2 was captured as $CaCO_3$ at the reaction starting point. After 5 min, most of the absorbed CO_2 was captured into the aqueous phase without forming as $CaCO_3$. The XRD analysis clarified the influence of carbonation on the crystalline phase. In addition, direct mineral carbonation of concrete fines under atmospheric pressure and 14% CO_2 was studied using different solid−liquid ratios (i.e., 10, 25, and 50 g/L). It was found that the CO_2 uptake efficiency was slightly higher when the solid−liquid ratio increased, which is different from the results presented in previous literature. The reason is attributable to the slow CO_2 dissolution reaction and carbonated particle collisions. In addition, comprehensive characteristic analyses of the carbonated products were undertaken. The TG analysis demonstrated that the degree of carbonation became higher as the solid−liquid ratio increased, corresponding to the results of CO_2 uptake. In addition, analysis of the PSD was conducted. When the solid−liquid ratio increased, the average particle size reduced and the peak of the smaller particle size increased. TG analysis of the large and small carbonated particles demonstrated that the small carbonated particles had higher $CaCO_3$ concentration, confirming that the controlling mechanisms are carbonated particle collision and oversaturated precipitation. Furthermore, the effect of carbonation with different concentrations of introduced CO_2 was confirmed. The results showed that the case with a higher concentration of introduced CO_2 needed a higher solid−liquid ratio. This finding increases the possibility of developing a mineral carbonation reaction of concrete fines under conditions of low CO_2 concentration or a high solid−liquid ratio. The elemental composition and TCLP demonstrated that the carbonated products could potentially be used in several applications. Overall, the method of direct carbonation of concrete fines under atmospheric pressure shows considerable potential for CO_2 utilization without CO_2 pressurization. However, for industrial applications of the technique, further investigation is needed because the characteristics of actual waste concrete fines will vary owing to the impurities derived mainly from the contamination of the aggregates and different methods of production. The influence of impurities in actual waste concrete fines must be investigated in future work.

■ ASSOCIATED CONTENT

Supporting Information

The Supporting Information is available free of charge at https://pubs.acs.org/doi/10.1021/acsomega.0c00985.

Thermogravimetric analysis curves of the raw material and final carbonated products; scanning electron microscopy image of final carbonated products (PDF)

■ AUTHOR INFORMATION

Corresponding Authors

Hsing-Jung Ho − *Department of Environmental Studies for Advanced Society, Graduate School of Environmental Studies, Tohoku University, Sendai, Miyagi 980-0845, Japan;* orcid.org/0000-0002-6256-1589; Email: ho.hsing.jung.p4@dc.tohoku.ac.jp

Atsushi Iizuka − *Center for Mineral Processing and Metallurgy, Institute of Multidisciplinary Research for Advanced Materials, Tohoku University, Sendai, Miyagi 980-8577, Japan;* orcid.org/0000-0001-8186-9303; Email: atsushi.iizuka.e4@tohoku.ac.jp

Authors

Etsuro Shibata − *Center for Mineral Processing and Metallurgy, Institute of Multidisciplinary Research for Advanced Materials, Tohoku University, Sendai, Miyagi 980-8577, Japan*

Hisashi Tomita − *Business Development Department, Resources, Energy & Environment Business Area, IHI Corporation, Koto-ku, Tokyo 135-8710, Japan*

https://dx.doi.org/10.1021/acsomega.0c00985
ACS Omega 2020, 5, 15877−15890

Kenji Takano − *Business Development Department, Resources, Energy & Environment Business Area, IHI Corporation, Koto-ku, Tokyo 135-8710, Japan*

Takumi Endo − *Business Development Department, Resources, Energy & Environment Business Area, IHI Corporation, Koto-ku, Tokyo 135-8710, Japan*

Complete contact information is available at: https://pubs.acs.org/10.1021/acsomega.0c00985

Notes

The authors declare no competing financial interest.

■ ACKNOWLEDGMENTS

The authors thank James Buxton M.Sc. from Edanz Group (www.edanzediting.com./ac) for editing a draft of this manuscript.

■ REFERENCES

(1) Ho, H.-J.; Iizuka, A.; Shibata, E. Carbon Capture and Utilization Technology without Carbon Dioxide Purification and Pressurization: A Review on Its Necessity and Available Technologies. *Ind. Eng. Chem. Res.* **2019**, *58*, 8941−8954.

(2) Huang, C. H.; Tan, C. S. A Review: CO2 Utilization. *Aerosol Air Qual. Res.* **2014**, *14*, 480−499.

(3) Béarat, H.; Mckelvy, M. J.; Chizmeshya, A. V. G.; Gormley, D.; Nunez, R.; Carpenter, R. W.; Squires, K.; Wolf, G. H. Carbon Sequestration via Aqueous Olivine Mineral Carbonation: Role of Passivating Layer Formation. *Environ. Sci. Technol.* **2006**, *40*, 4802−4808.

(4) Abe, Y.; Iizuka, A.; Nagasawa, H.; Yamasaki, A.; et al. Chemical Engineering Research and Design Dissolution Rates of Alkaline Rocks by Carbonic Acid: Influence of Solid / Liquid Ratio, Temperature, and CO 2. *Chem. Eng. Res. Des.* **2012**, *91*, 933−941.

(5) Ghoorah, M.; Dlugogorski, B. Z.; Balucan, R. D.; Kennedy, E. M. Selection of Acid for Weak Acid Processing of Wollastonite for Mineralisation of CO2. *Fuel* **2014**, *122*, 277−286.

(6) Min, Y.; Li, Q.; Voltolini, M.; Kneafsey, T.; Jun, Y.-S. Wollastonite Carbonation in Water-Bearing Supercritical CO 2: Effects of Particle Size. *Environ. Sci. Technol.* **2017**, *51*, 13044−13053.

(7) Park, A.-H. A.; Jadhav, R.; Fan, L.-S. CO2 Mineral Sequestration: Chemically Enhanced Aqueous Carbonation of Serpentine. *Can. J. Chem. Eng.* **2003**, *81*, 885−890.

(8) Iizuka, A.; Sakai, Y.; Yamasaki, A.; Honma, M.; Hayakawa, Y.; Yanagisawa, Y. Bench-Scale Operation of a Concrete Sludge Recycling Plant. *Ind. Eng. Chem. Res.* **2012**, *51*, 6099−6104.

(9) Iizuka, A.; Honma, M.; Hayakawa, Y.; Yamasaki, A.; Yanagisawa, Y. Aqueous Mineral Carbonation Process via Concrete Sludge. *Kagaku Kogaku Ronbunshu* **2012**, *38*, 129−134.

(10) Iizuka, A.; Sasaki, T.; Honma, M.; Yoshida, H.; Hayakawa, Y.; Yanagisawa, Y.; Yamasaki, A. Pilot-Scale Operation of a Concrete Sludge Recycling Plant and Simultaneous Production of Calcium Carbonate. *Chem. Eng. Commun.* **2017**, *204*, 79−85.

(11) Lee, M. G.; Kang, D.; Jo, H.; Park, J. Carbon Dioxide Utilization with Carbonation Using Industrial Waste-Desulfurization Gypsum and Waste Concrete. *J. Mater. Cycles Waste Manage.* **2016**, *18*, 407−412.

(12) BenGhacham, A.; Pasquier, L. C.; Cecchi, E.; Blais, J. F.; Mercier, G. Valorization of Waste Concrete through CO2mineral Carbonation: Optimizing Parameters and Improving Reactivity Using Concrete Separation. *J. Cleaner Prod.* **2017**, *166*, 869−878.

(13) Iizuka, A.; Fujii, M.; Yamasaki, A.; Yanagisawa, Y. A Novel Reduction Process of CO2 Fixation by Waste Concrete Treatment. *Kagaku Kogaku Ronbunshu* **2002**, *28*, 587−592.

(14) Iizuka, A.; Fujii, M.; Yamasaki, A.; Yanagisawa, Y. Development of a New CO 2 Sequestration Process Utilizing the Carbonation of Waste Cement. *Ind. Eng. Chem. Res.* **2004**, *43*, 7880−7887.

(15) Katsuyama, Y.; Yamasaki, A.; Iizuka, A.; Fujii, M.; Kumagai, K.; Yanagisawa, Y. Development of a Process for Producing High-Purity Calcium Carbonate (CaCO3) from Waste Cement Using Pressurized CO2. *Environ. Prog.* **2005**, *24*, 162−170.

(16) Iizuka, A.; Yamasaki, A.; Yanagisawa, Y. Cost Evaluation for a Carbon Dioxide Sequestration Process by Aqueous Mineral Carbonation of Waste Concrete. *J. Chem. Eng. Japan* **2013**, *46*, 326−334.

(17) Shuto, D.; Nagasawa, H.; Iizuka, A.; Yamasaki, A. A CO 2 Fixation Process with Waste Cement Powder via Regeneration of Alkali and Acid by Electrodialysis. *RSC Adv.* **2014**, *4*, 19778−19788.

(18) Shuto, D.; Igarashi, K.; Nagasawa, H.; Iizuka, A.; Inoue, M.; Noguchi, M.; Yamasaki, A. CO2Fixation Process with Waste Cement Powder via Regeneration of Alkali and Acid by Electrodialysis: Effect of Operation Conditions. *Ind. Eng. Chem. Res.* **2015**, *54*, 6569−6577.

(19) Huntzinger, D. N.; Gierke, J. S.; Kawatra, S. K.; Eisele, T. C.; Sutter, L. L. Carbon Dioxide Sequestration in Cement Kiln Dust through Mineral Carbonation. *Environ. Sci. Technol.* **2009**, *43*, 1986−1992.

(20) Tamilselvi Dananjayan, R. R.; Kandasamy, P.; Andimuthu, R. Direct Mineral Carbonation of Coal Fly Ash for CO 2 Sequestration. *J. Cleaner Prod.* **2016**, *112*, 4173−4182.

(21) Ji, L.; Yu, H.; Wang, X.; Grigore, M.; French, D.; Gözükara, Y. M.; Yu, J.; Zeng, M. CO2sequestration by Direct Mineralisation Using Fly Ash from Chinese Shenfu Coal. *Fuel Process. Technol.* **2017**, *156*, 429−437.

(22) Ukwattage, N. L.; Ranjith, P. G.; Yellishetty, M.; Bui, H. H.; Xu, T. A Laboratory-Scale Study of the Aqueous Mineral Carbonation of Coal Fly Ash for CO2 Sequestration. *J. Cleaner Prod.* **2015**, *103*, 665−674.

(23) Ukwattage, N. L.; Ranjith, P. G.; Wang, S. H. Investigation of the Potential of Coal Combustion Fly Ash for Mineral Sequestration of CO2by Accelerated Carbonation. *Energy* **2013**, *52*, 230−236.

(24) Lakmali, U. N.; Ranjith, P. G.; Ukwattage, N. L.; Ranjith, P. G. Effect of Brine Saturation on Carbonation of Coal Fly Ash for Mineral Sequestration of CO_2. *Engineering Geology for Society and Territory*; Lollino, G.; Manconi, A.; Clague, J.; Shan, W.; Chiarle, M., Eds.; Springer International Publishing: Cham, 2015; Vol. *1*, pp 479−482.

(25) Ukwattage, N. L.; Ranjith, P. G.; Perera, M. S. A. Effect of Accelerated Carbonation on the Chemical Properties and Leaching Behaviour of Australian Coal Fly Ash, to Improve Its Use as a Compost Amendment. *Environ. Earth Sci.* **2016**, *75*, 1398.

(26) Ukwattage, N. L.; Ranjith, P. G.; Li, X. Steel-Making Slag for Mineral Sequestration of Carbon Dioxide by Accelerated Carbonation. *Measurement* **2017**, *97*, 15−22.

(27) Ghacham, A. B.; Pasquier, L. C.; Cecchi, E.; Blais, J. F.; Mercier, G. CO2 Sequestration by Mineral Carbonation of Steel Slags under Ambient Temperature: Parameters Influence, and Optimization. *Environ. Sci. Pollut. Res.* **2016**, *23*, 17635−17646.

(28) Eloneva, S.; Said, A.; Fogelholm, C. J.; Zevenhoven, R. Preliminary Assessment of a Method Utilizing Carbon Dioxide and Steelmaking Slags to Produce Precipitated Calcium Carbonate. *Appl. Energy* **2012**, *90*, 329−334.

(29) Kodama, S.; Nishimoto, T.; Yamamoto, N.; Yogo, K.; Yamada, K. Development of a New PH-Swing CO2 Mineralization Process with a Recyclable Reaction Solution. *Energy* **2008**, *33*, 776−784.

(30) Song, C. CO 2 Conversion and Utilization. *J. CO_2 Util.* **2002**, 2−30.

(31) Kaliyavaradhan, S. K.; Ling, T.-C. Potential of CO 2 Sequestration through Construction and Demolition (C&D) Waste—An Overview. *J. CO_2 Util.* **2017**, *20*, 234−242.

(32) Naraharisetti, P. K.; Yeo, T. Y.; Bu, J. Factors Influencing CO2 and Energy Penalties of CO2 Mineralization Processes. *ChemPhysChem* **2017**, *18*, 3189−3202.

(33) Teir, S.; Eloneva, S.; Zevenhoven, R. Production of Precipitated Calcium Carbonate from Calcium Silicates and Carbon Dioxide. *Energy Convers. Manag.* **2005**, *46*, 2954−2979.

(34) Abanades, J. C.; Allam, R.; Lackner, K. S.; Meunier, F.; Rubin, E.; Sanchez, J. C.; Yogo, K.; Zevenhoven, R.. Mineral Carbonation and Industrial Uses of Carbon Dioxide. In *IPCC Special Report on Carbon Dioxide Capture and Storage*; Eliasson, B.; Sutamihardja, R. T. M., Eds.; Cambridge University Press, 2005; pp 320−338.

(35) Wolff-Boenisch, D.; Gislason, S. R.; Oelkers, E. H. The Effect of Crystallinity on Dissolution Rates and CO2 Consumption Capacity of Silicates. *Geochim. Cosmochim. Acta* **2006**, 858−870.
(36) Oelkers, E. H. General Kinetic Description of Multioxide Silicate Mineral and Glass Dissolution. *Geochim. Cosmochim. Acta* **2001**, 3703−3719.
(37) Pan, S.; Chang, E. E.; Chiang, P. CO2 Capture by Accelerated Carbonation of Alkaline Wastes: A Review on Its Principles and Applications. *Aerosol Air Qual. Res.* **2012**, *12*, 770−791.
(38) Ganesan, N.; Nagar, A.; Nagar, A. Studies on Strength Characteristics on Utilization of Waste Materials As Coarse Aggregate in Concrete. *Int. J. Eng. Sci. Technol.* **2011**, *3*, 5436−5440.
(39) Osmani, M.. Construction Waste. In *Waste*; Letcher, T. M.; Vallero, D. A., Eds.; Academic Press, 2011; pp 207−218.
(40) US Environmental Protection Agency. Construction and Demolition Debris Generation in the United States, 2014; New York, 2016.
(41) Renforth, P. The Negative Emission Potential of Alkaline Materials. *Nat. Commun.* **2019**, *10*, No. 1401.
(42) Benhelal, E.; Zahedi, G.; Shamsaei, E.; Bahadori, A. Global Strategies and Potentials to Curb CO2 Emissions in Cement Industry. *J. Cleaner Prod.* **2013**, *51*, 142−161.
(43) Hasanbeigi, A.; Price, L.; Lin, E. Emerging Energy-Efficiency and CO2 Emission-Reduction Technologies for Cement and Concrete Production: A Technical Review. *Renewable Sustainable Energy Rev.* **2012**, *16*, 6220−6238.
(44) Vanderzee, S.; Zeman, F. Recovery and Carbonation of 100% of Calcium in Waste Concrete Fi Nes: Experimental Results. *J. Cleaner Prod.* **2018**, *174*, 718−727.
(45) Jan, T. HeidelbergCement: Strong Builder of Carbon Neutrality. International Cement Review, 2019.
(46) Hoshino, S.; Yamada, K.; Hirao, H. XRD/Rietveld Analysis of the Hydration and Strength Development of Slag and Limestone Blended Cement. *J. Adv. Concr. Technol.* **2006**, *4*, 357−367.
(47) Pane, I.; Hansen, W. Investigation of Blended Cement Hydration by Isothermal Calorimetry and Thermal Analysis. *Cem. Concr. Res.* **2005**, *35*, 1155−1164.
(48) Chang, E. E.; Pan, S. Y.; Chen, Y. H.; Tan, C. S.; Chiang, P. C. Accelerated Carbonation of Steelmaking Slags in a High-Gravity Rotating Packed Bed. *J. Hazard. Mater.* **2012**, *227−228*, 97−106.
(49) Uibu, M.; Kuusik, R.; Andreas, L.; Kirsimäe, K. The CO2 -Binding by Ca-Mg-Silicates in Direct Aqueous Carbonation of Oil Shale Ash and Steel Slag. *Energy Procedia* **2011**, *4*, 925−932.
(50) Stumm, W.; Morgan, J. J..*Aquatic Chemistry: Chemical Equilibria and Rates in Natural Waters*; John Wiley and Sons: New York, 1996.
(51) Ohtaki, H. *Crystallization Processes*; John Wiley and Sons: New York, 1998.
(52) Covington, A. K.; Bates, R. G.; Durst, R. A. Definition of PH Scales, Standard Reference Values, Measurement of PH and Related Terminology (Recommendations 1984). *Pure Appl. Chem.* **1985**, *57*, 531−542.
(53) Han, Y. S.; Ji, S.; Lee, P. K.; Oh, C. Bauxite Residue Neutralization with Simultaneous Mineral Carbonation Using Atmospheric CO2. *J. Hazard. Mater.* **2017**, *326*, 87−93.
(54) Jo, H. Y.; Kim, J. H.; Lee, Y. J.; Lee, M.; Choh, S. J. Evaluation of Factors Affecting Mineral Carbonation of CO 2 Using Coal Fly Ash in Aqueous Solutions under Ambient Conditions. *Chem. Eng. J.* **2012**, *183*, 77−87.
(55) Baciocchi, R.; Costa, G.; DiGianfilippo, M.; Polettini, A.; Pomi, R.; Stramazzo, A. Thin-Film versus Slurry-Phase Carbonation of Steel Slag: CO2uptake and Effects on Mineralogy. *J. Hazard. Mater.* **2015**, *283*, 302−313.
(56) Huijgen, W. J. J.; Witkamp, G.-J.; Comans, R. N. J. Mechanisms of Aqueous Wollastonite Carbonation as a Possible CO2 Sequestration Process. *Chem. Eng. Sci.* **2006**, *61*, 4242−4251.
(57) Perry, R. H.; Green, D. W.; Maloney, J. O. *Perry's Chemical Engineers' Handbook*; 7th ed.; McGraw-Hill: New York, 1997.
(58) Dri, M.; Sanna, A.; Maroto-Valer, M. M. Mineral Carbonation from Metal Wastes: Effect of Solid to Liquid Ratio on the Efficiency and Characterization of Carbonated Products. *Appl. Energy* **2014**, *113*, 515−523.
(59) Santos, R. M.; Bodor, M.; Dragomir, P. N.; Vraciu, A. G.; Vlad, M.; VanGerven, T. Magnesium Chloride as a Leaching and Aragonite-Promoting Self-Regenerative Additive for the Mineral Carbonation of Calcium-Rich Materials. *Miner. Eng.* **2014**, *59*, 71−81.
(60) Jo, H.; Lee, M.; Kang, D.; Jung, K.; Park, J.. *Calcium Carbonate Production from MSWI Fly Ash by Indirect Carbonation*. In The 26th Annual Conference of Japan Society of Material Cycles and Waste Management; Japan Society of Material Cycles and Waste Management: Fukuoka, 2015; pp 82−83.
(61) Santos, R. M.; François, D.; Mertens, G.; Elsen, J.; VanGerven, T. Ultrasound-Intensified Mineral Carbonation. *Appl. Therm. Eng.* **2013**, *57*, 154−163.
(62) Eloneva, S.; Teir, S.; Salminen, J.; Fogelholm, C. J.; Zevenhoven, R. Steel Converter Slag as a Raw Material for Precipitation of Pure Calcium Carbonate. *Ind. Eng. Chem. Res.* **2008**, *47*, 7104−7111.
(63) Pan, S. Y.; Chiang, P. C.; Chen, Y. H.; Tan, C. S.; Chang, E. E. Kinetics of Carbonation Reaction of Basic Oxygen Furnace Slags in a Rotating Packed Bed Using the Surface Coverage Model: Maximization of Carbonation Conversion. *Appl. Energy* **2014**, *113*, 267−276.
(64) Lekakh, S. N.; Rawlins, C. H.; Robertson, D. G. C.; Richards, V. L.; Peaslee, K. D. Kinetics of Aqueous Leaching and Carbonization of Steelmaking Slag. *Metall. Mater. Trans. B* **2008**, *39*, 125−134.
(65) Irfan, M. F.; Usman, M. R.; Rashid, A. A Detailed Statistical Study of Heterogeneous, Homogeneous and Nucleation Models for Dissolution of Waste Concrete Sample for Mineral Carbonation. *Energy* **2018**, *158*, 580−591.
(66) Quaghebeur, M.; Nielsen, P.; Horckmans, L.; VanMechelen, D. Accelerated Carbonation of Steel Slag Compacts: Development of High-Strength Construction Materials. *Front. Energy Res.* **2015**, *3*, 467.
(67) Salman, M.; Cizer, Ö.; Pontikes, Y.; Santos, R. M.; Snellings, R.; Vandewalle, L.; Blanpain, B.; VanBalen, K. Effect of Accelerated Carbonation on AOD Stainless Steel Slag for Its Valorisation as a CO2-Sequestering Construction Material. *Chem. Eng. J.* **2014**, *246*, 39−52.
(68) Ukwattage, N. L.; Ranjith, P. G. Accelerated Carbonation of Coal Combustion Fly Ash for Atmospheric Carbon Dioxide Sequestration and Soil Amendment: An Overview. *J. Pollut. Eff. Control* **2018**, *06*, 1−8.
(69) Mohara, G.; Iizuka, A.; Nagasawa, H.; Yamasaki, A.; Kumagai, K.; Yanagisawa, Y. Phosphorus Recovery from Wastewater Treatment Plant by Using Waste Concretes. *Kagaku Kogaku Ronbunshu* **2009**, *35*, 12−19.
(70) Mohara, G.; Iizuka, A.; Nagasawa, H.; Kumagai, K.; Yamasaki, A.; Yanagisawa, Y. Phosphorus Recovery from Wastewater Treatment Plants by Using Waste Concrete. *J. Chem. Eng. Japan* **2011**, *44*, 48−55.
(71) Iizuka, A.; Sasaki, T.; Hongo, T.; Honma, M.; Hayakawa, Y.; Yamasaki, A.; Yanagisawa, Y. Phosphorus Adsorbent Derived from Concrete Sludge (PAdeCS) and Its Phosphorus Recovery Performance. *Ind. Eng. Chem. Res.* **2012**, *51*, 11266−11273.
(72) Iizuka, A.; Takahashi, M.; Nakamura, T.; Yamasaki, A. Boron Removal Performance of a Solid Sorbent Derived from Waste Concrete. *Ind. Eng. Chem. Res.* **2014**, *53*, 4046−4051.
(73) Sasaki, T.; Iizuka, A.; Watanabe, M.; Hongo, T.; Yamasaki, A. Preparation and Performance of Arsenate (V) Adsorbents Derived from Concrete Wastes. *Waste Manage.* **2014**, *34*, 1829−1835.
(74) Sasaki, T.; Iizuka, A.; Honma, M.; Yoshida, H.; Hayakawa, Y.; Yanagisawa, Y.; Yamasaki, A. Phosphorus Recovery from Waste Water by a Continuous Flow Type Reactor with Phosphorus Adsorbent Derived from Concrete Sludge (PAdeCS). *Kagaku Kogaku Ronbunshu* **2014**, *40*, 443−448.
(75) Wu, J.; Iizuka, A.; Kumagai, K.; Yamasaki, A.; Yanagisawa, Y. Improvement of Desulfurization Performances of Waste Cement Particles by Acid Treatment. *Ind. Eng. Chem. Res.* **2009**, *48*, 3303−3307.
(76) Wu, J.; Iizuka, A.; Kumagai, K.; Yamasaki, A.; Yanagisawa, Y. Desulfurization Characteristics of Waste Cement Particles as a Sorbent in Dry Desulfurization. *Ind. Eng. Chem. Res.* **2008**, *47*, 9871−9877.
(77) Iizuka, A.; Ishizaki, H.; Mizukoshi, A.; Noguchi, M.; Yamasaki, A.; Yanagisawa, Y. Simultaneous Decomposition and Fixation of F-

https://dx.doi.org/10.1021/acsomega.0c00985
ACS Omega 2020, 5, 15877−15890

Gases Using Waste Concrete. *Ind. Eng. Chem. Res.* **2011**, *50*, 11808−11814.

https://dx.doi.org/10.1021/acsomega.0c00985
ACS Omega 2020, 5, 15877−15890